LANGMUIR Article
Cite This: Langmuir 2018, 34, 14597−14607
pubs.acs.org/Langmuir

Structure of Phospholipid Mixed Micelles (Bicelles) Studied by Small-Angle X-ray Scattering

Henriette G. Mortensen, Grethe V. Jensen,† Sara K. Hansen, Thomas Vosegaard, and Jan Skov Pedersen*

Department of Chemistry and Interdisciplinary Nanoscience Center (iNANO), Aarhus University, Gustav Wieds Vej 14, 8000 Aarhus C, Denmark

Supporting Information

ABSTRACT: Mixed phospholipid micelles (bicelles) are widely applied in nuclear magnetic resonance (NMR) studies of membrane proteins in solution, as they can solubilize these proteins and provide a membrane-like environment. In this work, the structure of bicelles of dihexanoyl phosphatidyl choline (DHPC) and dimyristoyl phosphatidyl choline (DMPC) at different ratios was determined by small-angle X-ray scattering (SAXS) at 37 °C. Samples with concentrations as applied for NMR measurements with 28 wt % lipids were diluted to avoid concentration effects in the SAXS data. The DMPC/DHPC ratio within the bicelles was kept constant by diluting with solutions of finite DHPC concentrations, where the concentration of free DHPC is the same as in the original solution. Absolute-scale modeling of the SAXS data using molecular and concentration constraints reveals a relatively complex set of morphologies of the lipid aggregates as a function of the molar ratio Q of DMPC to DHPC. At $Q = 0$ (pure DHPC lipids), oblate core−shell micelles are present. At $Q = 0.5$, the bicelles have a tablet-shaped core−shell cylindrical form with an ellipsoidal cross section. For $Q = 1$, 2, 3.2, and 4, the bicelles have a rectangular cuboidal structure with a core and a shell, for which the overall length and width increase with Q. At $Q = \infty$ (pure DMPC), there is coexistence between multilamellar structures and free bilayers. For $Q = 1$−4, the hydrocarbon core is relatively narrow and the headgroup thickness on the flat areas is larger than that of, respectively, pure DHPC and DMPC, suggesting some mixing of DHPC into these areas and staggering of the molecules. This is further supported by comparisons of the ratio of the areas of rim and flat parts and estimates of the composition of the flat areas.

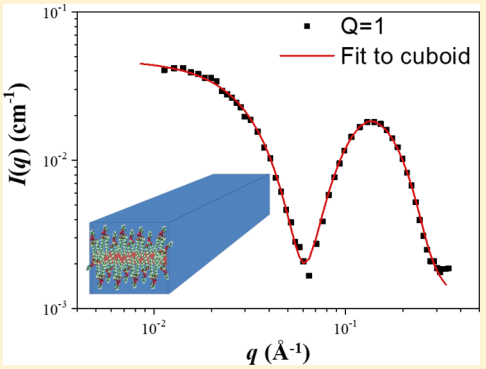

INTRODUCTION

Self-assembled, mixed phospholipid anisotropic micelles in water are normally referred to as bicelles. The name stems from the proposed structure of bilayered micelles, in short bicelles.[1] For bicelles of dihexanoyl phosphatidyl choline (DHPC) and dimyristoyl phosphatidyl choline (DMPC), it has been proposed that DMPC molecules with relatively long C14 hydrocarbon tails constitute a flat bilayer, whereas DHPC molecules with shorter C6 tails form a circular rim of the bicelles, leaving them disk shaped.[2,3] This model is in accordance with curvature arguments in terms of the critical packing parameter.[4] Short-chain DHPC has the lowest packing parameter and thus forms the curved part of the structure, whereas DMPC with a larger packing parameter forms the flat areas. According to this idealized picture, the DMPC/DHPC ratio (Q) determines the size of the bicelles. The bicelles are smallest for the idealized circular disk-shaped bicelles with complete segregation of DHPC and DMPC, and this gives the largest number of bicelles, which gives the maximum for the entropy of mixing with the solvent.

Despite an ongoing discussion on the morphology of bicelles, all studies agree that the lipids form some variation of a bilayer or micelle structure in water. The membrane-like structure of bicelles can solubilize membrane proteins, and because of their anisotropic morphology, they may align in a strong magnetic field. The combination of these properties makes them widely applied in nuclear magnetic resonance (NMR) studies of membrane proteins in solution.[5] In the present study, we use the word bicelle to describe the self-assembled structure of a mixture of DHPC and DMPC characterized by their mixing ratio within the bicelle, Q = [DMPC]/[DHPC], without associating the word bicelle with any specific structure. Throughout this paper, we refer to the head and the tail of DMPC and DHPC. The tail is defined as the two hydrocarbon chains (corresponding to 5 aliphatic carbons for each tail on DHPC and 13 for DMPC, as the carbon in the ester group is not included) and the head constitutes the rest of the molecule (see Figure 1 for molecular structure).

Received: August 9, 2018
Revised: October 28, 2018
Published: November 1, 2018

DOI: 10.1021/acs.langmuir.8b02704
Langmuir 2018, 34, 14597−14607

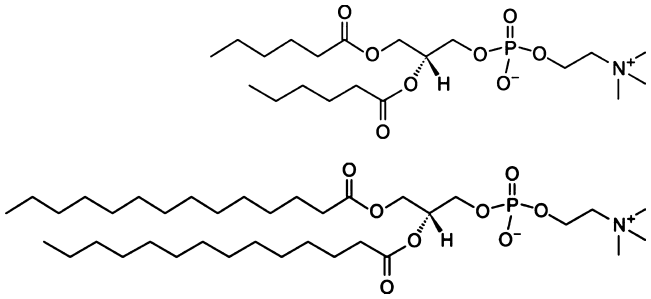

Figure 1. Top: DHPC. Bottom: DMPC.

In the following, a selection of morphologies reported in the literature is reviewed to illustrate the dependence on environmental and chemical parameters on the coassembled structures. van Dam et al.[3] used cryotransmission electron microscopy (cryo-TEM) and dynamic light scattering (DLS) and concluded that, when increasing Q or temperature, the morphology changes from isotropic particles to disks and then into slightly flattened cylinders that turn into branched, flattened cylinders and then into a perforated lamellar structure. In this study, van Dam et al. performed the experiments in 4-(2-hydroxyethyl)-1-piperazineethanesulfonic acid (HEPES) buffer and 150 mM NaCl. In a small-angle neutron scattering (SANS) study, Harroun et al.[6] reported a discoidal morphology below 20 °C, core−shell cylinders at 35 °C, and extended lamella at 45 °C for Q = 3.2 in pure water. In several studies,[6−8] bicelle samples were diluted (or simply prepared at low lipid concentrations) without paying the necessary attention to the high water solubility of the short-tail lipid, and the associated effect on the bicelle composition. Diluting with pure water leads to transfer of some of the short-tail lipids from the bicelle into the bulk, and thereby an (unintentional) change of the Q within the bicelles, which makes it hard to determine if morphology changes are directly related to dilution or in reality are an outcome of a compositional change within the bicelles. The temperature and concentration dependence makes it difficult to draw a general conclusion on the structure of bicelles. The present study aims to determine the shape and size of DMPC−DHPC bicelles in water for a range of mixing ratios Q = 0, 0.5, 1, 2, 3.2, 4, ∞, at 37 °C. The samples are diluted by water containing a certain concentration of "free", monomeric DHPC to keep the Q within the bicelles constant upon dilution from 28 to 0.2 wt %. The concentration of free DHPC in the samples can be determined experimentally using small-angle X-ray scattering (SAXS) due to the special scattering contrasts, as given by the excess electron densities, for the lipids. The two lipids (Figure 1) have hydrocarbon tails with negative excess electron density relative to that of water, whereas the headgroups have positive excess electron density. The overall ratio of negative to positive scattering is different for the two lipids, and for bicelles, this ratio thus depends on the composition. The SAXS data for core−shell structures in the present work with negative and positive scattering density contain pronounced minima and maxima (Figure S2). The angular position of these in the data depends on the overall ratio of negative to positive scattering and thus on the composition of the bicelles. Therefore, the dilution media with the correct DHPC concentration is the one where the position of the minima and maxima is independent of concentration. Note that free DHPC is not used in the dilution of pure DMPC and DHPC solutions. The structure of the bicelles is reported as determined by modeling of SAXS data, and confirmed by comparison with ^{31}P NMR data for the mixing ratio Q = 3.2.

MATERIALS AND METHODS

Sample Preparation. DHPC and DMPC were purchased in chloroform solution from Avanti Polar Lipids (Alabaster, AL). The lipid stock solution was prepared as follows: DMPC and DHPC were pipetted into separate vials and placed in a desiccator at a pressure below 1 mbar for the chloroform to evaporate. DMPC was solubilized in Milli-Q water by consistent stirring and gentle heating, which produced a milky solution. The solution became clear when DHPC was added. The solutions were frozen in liquid nitrogen for 30 s and then heated to 55 °C for 10 min. This temperature cycle was repeated 3−5 times to homogenize the viscous samples. After the last step, the bicelle solution was ready for dilution.

For each Q value, SAXS measurements were performed on samples with a total lipid weight percent of 0.2, 0.5, 1, 2, 5, 10, 20, and 28. On the basis of SAXS data from such a concentration series, it is possible to determine the concentration below which the structure factor effects (originating from interparticle interference effects) can be neglected. In the present work, the composition, Q, is defined as the molar ratio of DMPC to DHPC within the bicelles, and therefore, it is important to consider the high solubility of single molecules of DHPC in water when diluting the samples, and hence, the samples were diluted with an aqueous solution of DHPC. Because of the relatively long hydrocarbon chains of DMPC, its solubility in water as single molecules is very low and can be neglected. As mentioned, if the dilution media does not have the correct DHPC concentration, dilution will lead to a shift in the composition in the bicelles. As the solubility of DHPC is affected by the surroundings, and changes as a function of lipid composition, it is not straight-forward to determine what the appropriate DHPC concentration for a certain value of Q. Thus, dilutions with solutions of different DHPC concentrations were performed to find the concentration for which the position of the minimum in the data and the shape of the scattering pattern are unchanged by dilution. It should be noted that in order to model the SAXS data on absolute scale with molecular constraints, it is crucial that the composition of the bicelle is known. Data for the dilution series that fulfilled this requirement were applied for further structural modeling, specifically selecting the data set for a concentration of 2 wt %, which is the highest concentration where structure factor effects were not observed.

SAXS Instrumentation. The shape and size of the bicelles were studied by SAXS. The measured scattering intensity, $I(q)$, is a function of the modulus of the scattering vector q

$$q = 4\pi \sin(\theta)/\lambda \quad (1)$$

where λ = 1.54 Å is the X-ray wavelength and 2θ is the angle between the incident and scattered X-rays. The SAXS measurements were performed in a laboratory-based, two-pinhole, modified Bruker NanoStar instrument at the University of Aarhus.[9] The pinhole before the sample is a homebuilt scatterless slit system.[10] Normalization of data, subtraction of background, and calculation of pair distance distribution functions were done using the SUPERSAXS package (C. L. P. Oliveira and J. S. Pedersen, unpublished. Available upon request). All data were normalized to absolute-scale intensities of unit cm^{-1}, using a pure water sample as a standard.[9,11]

SAXS Data Analysis and Modeling. All data were background subtracted using data from the appropriate solvent solution, which for mixtures contains DHPC. All structural information was retrieved from 2 wt % data, where structure factor effects can be neglected (see Figure S2), while retaining good counting statistics for the form factor. Although absolute-scale modeling requires a good guess of the specific structure of the particle in solution, calculating the pair distance distribution function, $p(r)$, by indirect Fourier transformation (IFT)[12,13] only requires an initial guess on the largest dimension in the particle (D_{max}). The $p(r)$ function is a histogram of pair distances

DOI: 10.1021/acs.langmuir.8b02704
Langmuir 2018, 34, 14597−14607

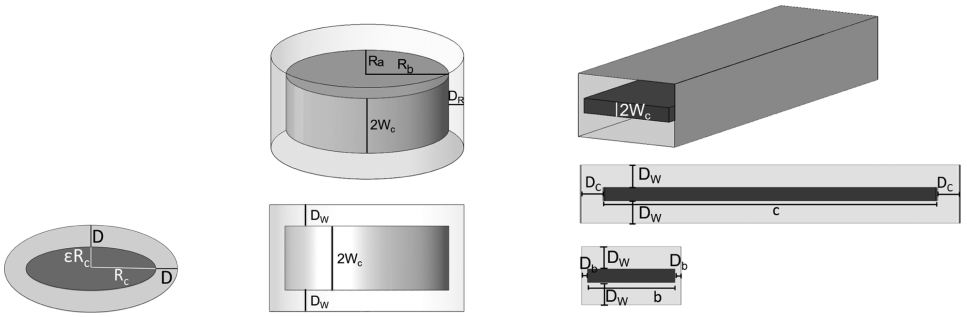

Figure 2. Model 1 (left): Core−shell ellipsoid. Model 2 (middle): Core−shell short cylinder with ellipsoidal cross section. Top: 3D representation. Bottom: Side view. Model 3 (right): Core−shell rectangular cuboid. Top: 3D representation. Middle: Side view. Bottom: Front view.

within the particle weighted by the scattering length density difference (SLDD; between particle and water) at the points that make up a pair, and therefore, this analysis provides direct real space information about the structures in solution. The resulting functions give D_{max} and a possible core−shell cross section can be recognized because of the negative contrast in the core and positive contrast in the shell, which give rise to an oscillation in the function at shorter distances.

To further determine the morphologies of the particles under investigation, absolute-scale model fitting was performed. Optimization of structural parameters in the models was done by a weighted least-square routine implemented in a home-written program). The program uses a reduced χ^2 parameter

$$\chi^2 = \sum_{i=1}^{N} \left(\frac{I_{exp}(q_i) - I_{mod}(q_i)}{s_i} \right)^2 \frac{1}{N - M} \quad (2)$$

for evaluating and optimizing the intensity in the models

$$I_{mod}(q) = nP(q)S(q) \quad (3)$$

where N is the number of data points, $I_{exp}(q_i)$ is the experimental intensity, $I_{mod}(q_i)$ is the model intensity, s_i is the statistical uncertainty on the ith experimental data point, M is the number of parameters defining the model intensity, n is the number density of particles, $P(q)$ is the form factor describing the structure of the particle, and $S(q)$ is the effective structure factor, which accounts for interparticle interaction effects. For data from the samples of lowest concentrations, which were applied here, it was not necessary to include a structure factor to successfully fit the data, except for data from pure DMPC samples. All models also include a fitted flat scattering background.

The SAXS data all show a pronounced and deep minimum (Figure S2), which is a result of the core−shell structure of the aggregates with negative scattering length density in the core and positive scattering length density in the shell. The sharp minima turned out to make it challenging to find models that can fit the data. Furthermore, the core−shell structures of the bicelles which can fit the data turned out to be anisotropic in shape, requiring a relatively large number of parameters for describing the structures. As the information content of the SAXS data is somewhat limited, the number of fitting parameters is kept as low as possible, while still having a model that gives a good fit to the data. Note that SANS studies of bicelles[14,15] are performed in D_2O solutions to have a good contrast. The use of D_2O in combination with nondeuterated lipids gives the same sign of contrast for the core and shell of the bicelles, and consequently, the SANS data contain less information than the SAXS data, and therefore, it is easier to fit the SANS data.

In the present work, a large number of geometrical models based on suggested structures for the bicelles were tested for fitting the SAXS data. However, many of these did not provide satisfactory fits to the data or were not able to give meaningful results while meeting the molecular constraints regarding contrasts and concentrations. It was concluded that four different (but related) models were required to fit the data sets for the seven different values of Q. These models 1−3 are on absolute scale using constraints for the following quantities: concentration of bicelles, concentration of monomeric DHPC, molecular weight (M_w) of lipids, volume of head (V_{head}) and tail (V_{tail}), electron density of head ($\rho_{e,head}$) and tail ($\rho_{e,tail}$), and the ratio between DMPC and DHPC (Q). Details of models, form factors, and model parameters are given in the Supporting Information. It is principally impossible to prove the uniqueness of the models. However, the use of molecular and concentration constraints makes it very challenging to find models that fit the data, and accordingly, other models that may fit the data equally well are likely to be quite similar in the overall structure but may vary a little in the details (e.g., have rounded edges and corners). In the following, a short description of each of the used model is given.

Model 1 (used for pure DHPC, $Q = 0$) is a core−shell ellipsoid based on the form factor of an ellipsoidal of revolution,[16] where core radius, R_c, and eccentricity, ε, of the core are fitted together with the thickness of the shell, D. A smearing factor for smearing the core−shell and shell−solvent interfaces is included with a fixed interface smearing width parameter, σ. The lipid molecules are divided into tail and head, so that the tails constitute the core with a low electron density and the heads constitute the shell with a higher electron density. It should be noted that it is mainly the phosphatidyl part that contributes to the contrast of the headgroup, whereas electron density of the choline part is very close to that of water. The fraction of water in the shell, F_w, and the aggregation number, N_{agg}, are derived from the fit parameters together with the constraints.

Model 2 (used for $Q = 0.5$) is a flat core−shell cylinder with an ellipsoidal cross section based on the form factor of an ellipsoidal cylinder,[17] where the fitting parameters are the radii of the core, R_a and R_b, the height of the core, $2W_c$, the thickness of shell, D_W, and the thickness of rim, D_R (see Figure 2, middle). Smearing widths for the core−shell and the shell−solvent interfaces, σ_i and σ_o (similar to model 1), are fixed. In this model, the electron densities reflect a core composed of the hydrocarbon tails of DHPC and DMPC and a shell composed of headgroups from both molecules. F_w and N_{agg} are derived from the resulting fit parameters together with the constraints.

Model 3 (used for $Q = 1$, 2, 3.2, and 4) is a core−shell rectangular cuboid based on the form factor given in ref.[18] A rectangular cuboid has the shape of a cigar box as shown in Figure 2, right. The geometrical fitting parameters are thickness of core, $2W_c$, width of core, b, length of core, c, thickness of bilayer shell, D_W, thickness of side shell, D_b, and thickness of end cap shell, D_c. Smearing widths for the core−shell and the shell−solvent interfaces, σ_i and σ_o, are fixed.

The simplest core−shell model would have the hydrocarbon chains from both DHPC and DMPC in the core and the headgroups in the shells; however, this model did not fit the data satisfactory. Therefore, another model was formulated with a core consisting of DHPC tails and the end of the DMPC tails (five carbons from each tail counting from the end of the molecule) and a shell consisting of headgroups plus the "rest" of the DMPC tails (see Figure S1). For the data sets with $Q = 1$ and $Q = 4$, it was necessary to fit the position of the DMPC molecules with respect to the core−shell interface. This was introduced through the fitting parameter F, which denotes the fraction of the "rest" that is moved from the shell to the core. Note that in order to reproduce the deep minima in the SAXS data, the shell

DOI: 10.1021/acs.langmuir.8b02704
Langmuir 2018, 34, 14597−14607

thickness of the ends and the sides had to be much smaller than the thickness of the shell at the flat parts (see Results and Discussion section for further details). Elongated micellar-like structures as those described by the present model are expected to have significant length polydispersity,[19] but as the models without inclusion of this already provided good fits to the data, the effect of polydispersity was not included.

Model 4 (used for pure DMPC, $Q = \infty$) is a combination of a multilamellar structure composed of bilayers and free bilayers inspired by the paper by Pabst et al.[20] using modified Caillé theory for describing the layered ordering of the multilayer stacks. For each bilayer, a core−shell structure described by box functions with interfacial smearing of the core−shell and shell−solvent interfaces was used. The fitting parameters are the scaling for the bilayer and multilayer contributions, Sc_{bi} and Sc_{mul}, respectively, the half-width of the core W_c, the shell thickness, D_W, and the SLDD of the shell relative to that of the core, $\Delta\rho_{shell}/\Delta\rho_{core}$, the repeat distance between stacks, d, a parameter controlling the shape of the peaks, η, the number of bilayers in the a multilamellar stacks, N, the width of polydispersity in the number of layers, σ_N, and a flat scattering background. The width of the smearing of the core−shell and shell−solvent interfaces, σ_C and σ_H, was kept fixed. This model is not on absolute scale, as it is crucial to know the exact concentration in solution, when using an absolute-scale approach in order to get reliable results and with structures as large as these (multilayered with close to 11 bilayers), the risk of sedimentation is large.

Bilayer Cross Section Profiles. Radial profiles of the excess electron densities corresponding to each of the structural models can be calculated by Fourier transforms of the scattering amplitudes, $A(q)$. For the oblate ellipsoid for $Q = 0$ (pure DHPC solution), the profile is obtained by a sine transform[21]

$$\Delta\rho(r) = \frac{1}{2\pi^2 r}\int_0^\infty A(q) q \sin(qr)\, dq$$

In order to obtain the structure in the direction perpendicular to the flattened micelle, the amplitude from this direction is used. For the lamellar structures, the profile is obtained by a cosine transform[21]

$$\Delta\rho(r) = \frac{1}{2\pi}\int_0^\infty A(q) \cos(qr)\, dq$$

Here, the amplitude for the direction perpendicular to the flat areas of the models is used. For ease of comparison, the profiles were normalized to $\Delta\rho(r = 0) = -1$.

NMR Experiments. All NMR experiments were performed at 37 °C on a Bruker Avance II spectrometer with a 9.4 T magnet corresponding to a ^{31}P resonance frequency of 161.9 MHz employing single-pulse excitation, continuous-wave decoupling (15 kHz) during the 20 ms long acquisition time, a repetition delay of 3 s, and with the following number of scans (wt %): 4 (28), 4 (20), 16 (10), 64 (5), 256 (2), 1024 (1), 4096 (0.5), and 16384 (0.2).

Interpretation of NMR Data. To address structures applied for NMR studies of membrane proteins, it is most interesting to discuss bicelles with $Q \gtrsim 2$. The large bicelles formed at these compositions show a high degree of alignment in a strong magnetic field.[22] This allows obtaining direct information on the geometry and orientation of the bicelles from the NMR experiments. A lipid bilayer oriented with its bilayer normal parallel to the magnetic field displays a single ^{31}P peak at $\delta_\parallel = 33$ ppm,[23−25] with the precise frequency determined by the geometry of the sample.[25,26] Magnetically oriented bicelles have the bilayer normal perpendicular to the magnetic field.[2,27] As the chemical shift is a second-rank tensorial interaction, the observed chemical shift scales with a second-order Legendre polynomial, $(3\cos^2\theta - 1)/2$, where $\theta = 0°$ is for a parallel orientation and $\theta = 90°$ is for a perpendicular orientation. Hence, by a simple geometrical consideration, one would expect the ^{31}P chemical shift of the bilayer part of the bicelle with its bilayer normal perpendicular to the magnetic field to be $\delta_{bilayer} = -\delta_\parallel/2 = -16.5$ ppm.[26] In contrast, spherical micelles are small isotropic moieties, which display an isotropic chemical shift of ∼0 ppm,[28] like free lipids in solution. Any deviations from these shifts will potentially carry important information on the lipid system.

Bicelle solutions with $Q \gtrsim 2$ display two important differences from the situation described above: (i) there is no peak at 0 ppm, but rather a peak at $\delta_{res} \approx -5$ ppm, typically attributed to the short-chain lipids residing at the rim of the bicelle,[2] and (ii) the peak of the bilayer part is shifted from −16.5 ppm to approximately −10 to −13 ppm. This deviation is normally explained by the oriented bicelle having an order parameter of $S^2 \approx 0.8$,[29] leading to a reduction of the frequency to $\delta_{bilayer} = -S^2\delta_\parallel/2 \approx -13.2$ ppm. The fact that no peak is observed at the isotropic chemical shift (0 ppm) implies that the short-chain lipids in solution must be in rapid exchange with lipids in the bicelles displaying some alignment, as a fast exchange (with a rate $k \gg \nu_0\Delta\delta$, where ν_0 is the ^{31}P Larmor frequency and $\Delta\delta$ is the chemical shift difference between the exchanging components. Here, this implies that the short-chain lipids exchange with a rate $k \gg 10^3$ s^{-1}, which is reasonable) will lead to observation of a single peak with a resonance frequency corresponding to the weighted average frequency.[30] That is, if two moieties A and B with populations P_A and P_B resonate at frequencies δ_A and δ_B, the observed resonance will be at $\delta = (P_A\delta_A + P_B\delta_B)/(P_A + P_B)$. Note that in the present work, the aim is not to establish a measure of the bilayer kinetics but to limit the discussion to moieties in fast exchange and moieties without exchange.

RESULTS AND DISCUSSION

Determining the Correct Dilution Media. On the basis of the scattering data for each dilution series (see Figure S2), the appropriate concentration of DHPC in the dilution media was determined for each Q value. The best results were obtained with the following values: for $Q = 0.5$, 9 mM DHPC; $Q = 1$ and 2, 5 mM DHPC; and $Q = 3.2$ and 4, 4.5 mM DHPC. As Q decreases, the DHPC concentration in the dilution media increases but stays below the critical micelle concentration of pure DHPC of 14−15 mM.[31,32] The result is close to what is found by Ottiger and Bax[33] for $Q = 3.5$ (which is equivalent to an effective Q of 5.1 in the bicelles according to their own results). They conclude that diluting $Q = 3.5$ (5.1) with a 5−6 mM DHPC solution prevents the formation of large light-scattering particles. Others[34,35] have investigated systems of lower Q and conclude that 7 mM is the appropriate DHPC concentration for the dilution media for $Q \approx 0.5$, close to the result in this study of 9 mM. It should be noted that these studies[34,35] were performed in an acetate buffer and that one of the studies[34] concerns POPC−DHPC micelles rather than DMPC−DHPC.

Model-Independent Structural Results (IFT Analysis). The $p(r)$ functions in Figure 3 show that the composition of DHPC and DMPC (Q) influences the morphology in a number of ways. For the pure DHPC system, the oscillating behavior of the $p(r)$ function at small r confirms that the self-assembled particles in the solution have a core with a negative SLDD and a shell/corona with a positive SLDD. The overall particle size, given by D_{max}, is 50 Å. Introducing DMPC into the system (Figure 3) gives rise to a more pronounced oscillation in $p(r)$ and a larger D_{max} of 70 Å, indicating a larger core and therefore a larger micelle in accordance with the longer hydrocarbon chains of the DMPC molecule. When the DMPC concentration is further increased (the total lipid concentration is constant at 2 wt % for these SAXS data) to yield $Q = 1−4$, the characteristics of $p(r)$ functions is unaltered at low distances r, but D_{max} continues to increase. For these samples, a linear decrease in $p(r)$ is observed at larger r (disregarding the ripples due to minor numerical problems with the computational method used). This is a known characteristic for a rodlike particle.[21]

DOI: 10.1021/acs.langmuir.8b02704
Langmuir 2018, 34, 14597−14607

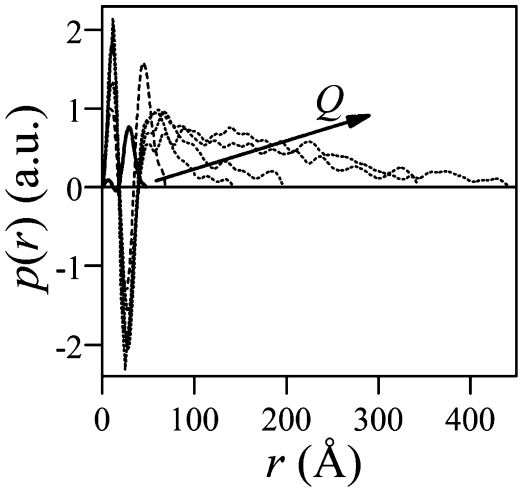

Figure 3. $p(r)$ functions for pure DHPC and DMPC/DHPC mixtures Q = 0.5–4. DHPC (solid line), Q = 0.5 (dashed line), Q = 1–4 (dotted line).

Particle Morphology Obtained by Absolute-Scale SAXS Data Modeling. To get detailed information of the particle shape, cross section, and aggregation number, SAXS data for 2 wt % samples were modeled on absolute scale. For Q = 3.2, ^{31}P NMR data are also presented and discussed.

DHPC Micelles. The SAXS data for the DHPC sample (Figure 4, top) were modeled using the form factor of a core–shell oblate ellipsoid (model 1). The best fit was obtained for an oblate core. The radius of the core R_C is 15.5 ± 0.1 Å, the core eccentricity ε is 0.33 ± 0.01, the thickness of the shell D is 4.70 ± 0.07 Å, and the derived aggregation number is 16. The detailed results and errors are given in Table 1. The results are in accordance with the findings from the IFT analysis, which revealed a relatively small core–shell particle. In the narrow direction, the core radius is 5.2 Å, which is reasonable for the C5 chains of DHPC. Note that for the headgroup, it is mainly the phosphatidyl group, which is visible, which agrees with the small width of the shell of 4.7 Å. A similar shell thickness was determined by Lipfert et al.[36] in their SAXS study.

In an SANS study by Lin et al.,[37] DHPC data were fitted with a model of prolate micelles of similar size and similar aggregation number of 19. As noted in ref 38., prolate and oblate micelle models can give similar quality of fits to small-angle scattering data, so it is quite difficult to distinguish the two shapes. The aggregation number is slightly lower than the values of 35–40 as determined by Lipfert et al.[36] and in closer agreement with our result.

***Q* = 0.5.** SAXS data for the sample with a Q ratio of 0.5 (Figure 4, middle) were modeled using model 2, which is a core–shell cylinder with an ellipsoidal cross section (Figure 2). The core radii R_a and R_b are fitted to 14.6 ± 0.2 and 24.4 ± 0.4 Å, respectively, the half-thickness of the core W_c is 9.2 ± 0.1 Å, the thickness of the shell is 3.7 ± 0.2 Å in both directions (D_W and D_R parameters), and the aggregation number is 66. A half the width of the core of 9.2 Å is reasonable for the C13 chains of DMPC. The shell is quite narrow and this suggests a very well-defined layer of the phosphatidyl group both on the flat part and at the rim. Note that the geometrical dimensions make this structure resemble a disk rather than a cylinder. The detailed results and errors are given in Table 1. The obtained particle size is in agreement with the results from DLS studies[3,35] for Q = 0.5, which concludes a discoidal

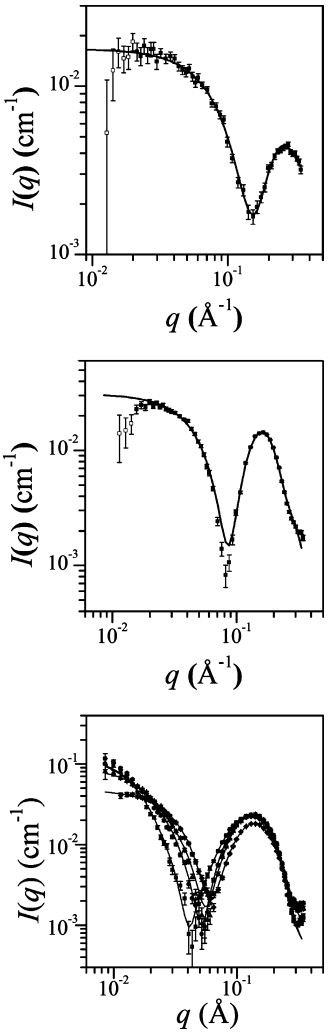

Figure 4. Top: Experimental SAXS data for 2 wt % pure DHPC. Solid squares are data used in the fit. Line shows fit by model 1 (core–shell ellipsoid). Middle: Experimental SAXS data for 2 wt % Q = 0.5. Solid squares are data used for the fit. Line shows fit by model 2 (core–shell short cylinder with ellipsoidal cross section). Bottom: Experimental SAXS data for 2 wt % Q = 1, 2, 3.2, and 4 given by diamonds, triangles, spheres, and squares, respectively. The solid lines are the fits by model 3 (core–shell rectangular cuboids).

morphology in agreement with the present SAXS results. It should be noted that these light-scattering results were obtained for samples in HEPES or acetate buffer and with added NaCl, whereas the current study is performed in water with DHPC as the only additive. Ye et al.[39] also conclude the formation of small micelles of similar size but argues that the morphology depends on the concentration and that mixed, spherical micelles are formed at a low (75 mM) lipid concentration and "classical" discoidal, segregated (DMPC forming bilayer and DHPC forming rim) bicelles are formed at a higher concentration (150 mM). As the given Q value (0.5) is not controlled during dilution in the study by Ye et al., the real Q value within the bicelles is higher in the most dilute sample, and this, rather than a concentration effect, might be the reason for the morphology variation that they observe. In the current study, using absolute-scale modeling of SAXS data, it was not possible to make a model, which could directly reveal if the particle is segregated, as the headgroup electron

DOI: 10.1021/acs.langmuir.8b02704
Langmuir 2018, 34, 14597–14607

Table 1. Parameters Obtained by Model Fits to SAXS Data for Pure DHPC, Q = 0.5, and Pure DMPC

pure DHPC (model 1)		Q = 0.5 (model 2)		pure DMPC (model 4)	
R_C [Å]	15.5 ± 0.1	R_a [Å]	14.6 ± 0.2	W_c [Å]	9.1 ± 0.4
ε	0.33 ± 0.01	R_b [Å]	24.4 ± 0.4	D_W [Å]	12.3 ± 0.6
D [Å]	4.70 ± 0.07	W_c [Å]	9.2 ± 0.1	$\Delta\rho_{head}$	−1.24 ± 0.11
σ [Å]	1.5	D_W [Å]	3.7 ± 0.2	σ_C [Å]	2.0 (fixed)
F_w	0.54	D_r [Å]	3.7 ± 0.2	σ_H [Å]	2.0 (fixed)
N_{agg}	16	σ_i [Å]	3.0 (fixed)	d [Å]	61.7 ± 0.1
c-cmc [g/L]	18.9	σ_o [Å]	3.0 (fixed)	η	0.087 ± 0.002
χ^2	0.9	F_w	0.15	N	10.7 ± 0.2
		N_{agg}	66	σ_N	1.7 ± 2.2
		c [g/L]	20.4	χ^2	6.8
		χ^2	11.1		

density is identical for DMPC and DHPC. However, the narrow headgroup shell suggests a high degree of segregation.

Q = 1, 2, 3.2, and 4. Results from samples of Q = 1−4 are presented together as the data from these (Figure 4) were modeled by the same model (model 3), describing a core−shell rectangular cuboid. The modeling results (Table 2) are in

Table 2. Parameters Obtained by Model Fits to SAXS Data Q = 1, 2, 3.2, and 4

model 3	Q = 1	Q = 2	Q = 3.2	Q = 4
W_c [Å]	4.8 ± 0.1	5.9 ± 0.1	6.1 ± 0.1	6.5 ± 0.1
b [Å]	55 ± 2	58 ± 2	76 ± 2	157 ± 13
c [Å]	111 ± 6	238 ± 21	370 ± 21	301 ± 41
D_a [Å]	21.4 ± 0.1	19.9 ± 0.1	19.4 ± 0.2	17.7 ± 0.2
D_b [Å]	1.7 ± 0.5	2.8 ± 0.3	2.6 ± 0.3	2.1 ± 0.9
D_c [Å]	1.7 (fixed)	2 (fixed)	1.5 (fixed)	1.5 (fixed)
F	0.164	0	0	0.6
σ_i [Å]	1 (fixed)	1 (fixed)	2 (fixed)	2 (fixed)
σ_o [Å]	3 (fixed)	2 (fixed)	2 (fixed)	2 (fixed)
F_w	0.7	0.5	0.4	0.7
N_{agg}	158	487	1041	1151
c [g/L]	18.7	19.7	19.3	19.5
χ^2	4.5	5.6	8.1	7.3

accordance with the results from the IFT analysis which gives a rodlike core−shell morphology that grows in length with increasing Q while maintaining its overall shape characteristics. Values of most of the fitting parameters are given in Table 2. The core thickness is similar for all values of Q. The entire tail groups of DHPC and the corresponding five terminal hydrocarbons of DMPC all contribute to the core. The parameter F determines the fraction of the remaining part of the DMPC tails (referred to as "the rest") that contributes to the core (see Supporting Information model 3 for further explanation). The best fits were obtained when F = 0.16 for Q = 1, F = 0 for Q = 2 and Q = 3.2, and F = 0.6 for Q = 4. The high F value for Q = 4 reflects the high DMPC content, which in turn leads to a larger hydrocarbon core. The shell contains the headgroups of both DHPC and DMPC, as well as a part of the DMPC tails as described above. The core thickness $2W_c$ is smaller than for Q = 0.5 and increases with Q for Q = 1−4, indicating that DMPC and DHPC have some degree of mixing. If this was not the case, the core thickness should be independent of Q, as only DMPC would form the bilayer and DHPC the rim. The thickness of the shell in the W_c direction, D_W, decreases slightly with Q. It is significantly larger (18−21 Å) than the shell thickness obtained for Q = 0.5 (3.7 Å) and also larger than that of pure DMPC bilayers (12.3 Å, see next section). For the extended structure for Q = 1−4 and pure DMPC, the large coherence length of the X-rays leads to lateral averaging of the profiles, and because of thermal fluctuations, this leads to some broadening. However, the larger headgroup width for the mixtures suggests some degree of intermixing of DHPC into the flat area of the bicelle, inducing some disorder and staggering of the molecules. Note again that it is mainly the phosphatidyl group which is visible and it is thus the distribution of the phosphatidyl which is described by the headgroup shell. The width, b, of the cuboids increases significantly above Q = 2 and the length of the cuboids is steadily increased throughout the Q range. The shell thicknesses in the b and c directions (D_b and D_c) are quite small, reflecting that only a few molecules are positioned at the edges of the bicelles. As for the Q = 0.5 case, comparison with other studies must be done with care. First of all, the majority of the bicelle literature cannot be used for comparison as they are for experiments performed at temperatures below the DMPC melting temperature (and not at 37 °C as used in the present work). Second, solvent conditions (buffer and salts) vary a lot within the studies, and as the present work was performed in water with small amounts of singly dissolved DHPC, direct comparison is difficult. Some dependence of solvent conditions can be expected because both lipids, despite being zwitterionic, have charges, and therefore, electrostatic interactions and screening effects may play a role for the morphology of the bicelles. However, a few studies are performed under conditions that are relatively close to the ones applied in the present study. Ye et al.[39] observed flat band-like structures (a morphology closely related to rectangular cuboids) at Q = 1.5 and 37 °C using cryo-TEM; however, no information is given on bicelle size and the experiments were performed in phosphate buffer. Nieh et al.[15] modeled Q = 3.2 SANS data measured at 45 °C as cylinders but concludes that the morphology must be closer to ribbons (again a morphology closely related to rectangular cuboids) because of the tendency of DMPC to form bilayers. van Dam et al.[3,8] also reported flattened cylinders. However, the solvent conditions in the van Dam study were also different (HEPES and 150 mM NaCl[3] or 10 mM sodium phosphate buffer and 0.01% NaN_3[8]) from the present study. An NMR study by Sanders and Schwonek[40] concluded that the studied bicelles had a discoidal morphology, but the data that this conclusion is based on are also compatible with a rectangular cuboid model. Sanders and Schwonek state that the ability to orient in a magnetic field is not necessarily related to a discoidal morphology, but that it may also originate from a cylindrical

DOI: 10.1021/acs.langmuir.8b02704
Langmuir 2018, 34, 14597−14607

morphology. In the publication, the latter hypothesis is turned down with the argument that cylinders are not bilayered. However, rectangular cuboids are in fact bilayered while having a rodlike character, meaning that our results are in accordance with the results of Sanders and Schwonek.[40]

Comparison with NMR results for Q = 3.2. To allow direct comparison of NMR and SAXS data, the fact that SAXS samples employ 2 wt % lipids in the samples, while NMR samples may use up to 30 wt % lipids for sensitivity reasons,[41] needs to be addressed. To link these extremes, bicelle samples with lipid concentrations of 0.2, 0.5, 1, 2, 5, 10, 20, and 28 wt % were also prepared for NMR experiments. All samples targeted a ratio of Q = 3.2, using a concentration of free DHPC of 4.5 mM for the dilution. The ^{31}P spectra of these samples are shown in Figure 5. All spectra contain as expected two

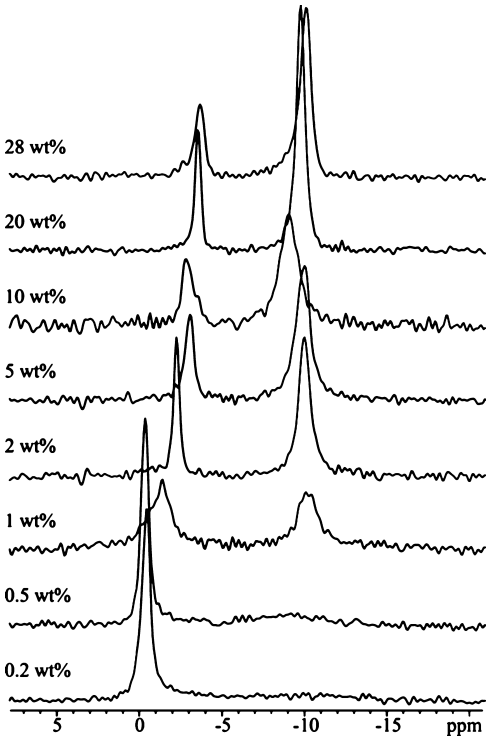

Figure 5. ^{31}P NMR spectra at 37 °C for different lipid concentrations and Q = 3.2.

peaks, henceforth referred to as the bilayer peak and the residual peak. The bilayer peak in samples with low lipid concentrations broadens substantially, although it remains at approximately the same frequency. The broadening may be caused by a lower degree of alignment of the dilute bicelles as compared to concentrated bicelles, where cooperative alignment effects may be expected.

The intensity ratio between the bilayer and residual peaks versus the concentration of lipid for the different samples is shown in Figure 6a. Note that the error bars are quite large compared to the variations across the samples; hence, no strong conclusions based on the intensities will be made. Assuming that all long-chain lipids primarily reside in the bilayer part, whereas the short-chain lipids primarily reside in the solution and rim of the bicelle, a plot of the concentration ratio between long-chain and short-chain lipids (C_{long}/C_{short}, not to be confused by Q within the bicelle) should fit the intensity ratio. This ratio is indicated by a solid line in Figure

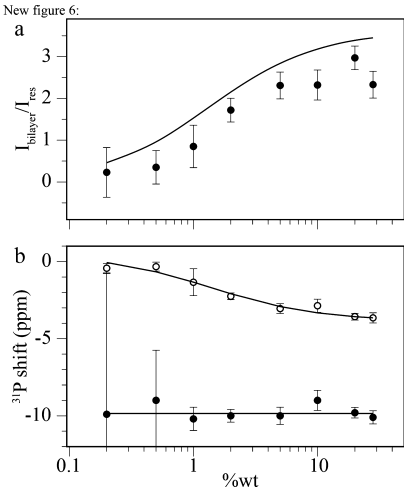

Figure 6. (a) Relative intensities (filled circles) and concentration ratio (solid line) and (b) chemical shifts for the bilayer and residual peaks in the ^{31}P NMR spectra in Figure 5. In (b), open circles represent the residual peaks and filled circles represent the bilayer peaks. The line are fits to the residual peaks as described in the text and to the bilayer peaks by a constant.

6a and shows that this model slightly overestimates the intensity ratio but still represents the essential trends of the data.

More interestingly, the frequency change for the two peaks is plotted Figure 6b. The bilayer peak is located at $\delta_{bilayer} = -9.9 \pm 0.5$ ppm and does not show any systematic variation with the lipid concentration. On the other hand, the peak for the residual lipids moves from −3.7 to −0.3 ppm, when going from concentrated to dilute samples. The residual peak arises from molecules (mainly short-chain lipids) either in solution or bound in the rim of the bicelle. As explained above, as only one peak is observed, the molecules are in a fast exchange between these states. These states will be associated with the ^{31}P chemical shifts δ_{sol} and δ_{rim}. The concentration of free DHPC in the solution, C_{sol}, is assumed constant (=4.5 mM) as explained above, and the total concentration of DHPC in the samples, C_{short}, can be calculated directly for all dilutions. The resonance frequency of the residual peak may be written as

$$\delta_{res} = \frac{C_{sol}}{C_{short}}\delta_{sol} + \frac{C_{short} - C_{sol}}{C_{short}}\delta_{rim}$$

Using this equation, it is found that the experimentally measured values for δ_{res} may be fitted best with the values of $\delta_{rim} = -4.7 \pm 0.2$ ppm and $\delta_{sol} = 0.5 \pm 0.2$ ppm. The value for δ_{sol} is in good agreement with previous findings for monomeric DHPC,[8,23,27,42−44] and the fact that δ_{rim} is approximately scaled by a factor −0.5 compared to $\delta_{bilayer}$ is in good agreement with typical observations.

To conclude, the NMR investigation does not suggest the presence of short-chain lipids in the bilayer part of the bicelles. This is supported by previous ^{2}H NMR studies of bicelles, where either the short- or long-chain lipids were ^{2}H labeled.[42,45] These studies revealed that quadrupolar splitting for the side chains of the short-chain lipids was much smaller than for the long-chain lipids, suggesting that only the long-chain lipids reside in the bilayer part. We have performed similar ^{2}H NMR studies on the present samples (data not shown) and obtained similar results. It should be noted that our data cannot be used to completely exclude the presence of

DOI: 10.1021/acs.langmuir.8b02704
Langmuir 2018, 34, 14597−14607

short-chain lipids in the bilayer part. These lipids may indeed be present in the bilayer part, but they will be in fast exchange with the short-chain lipids in the solution and thereby be part of the "remaining" NMR peak. It has been suggested that such a presence will be more pronounced at higher temperatures.[23,42] Overall, the characteristics of the NMR spectra are in good agreement with the proposed bicelle model 3 for the investigated Q = 3.2 bicelles.

DMPC Multilayers. SAXS data from pure DMPC solution are remarkably different from the data for the other samples (Figure 7). The presence of two peaks shows that the structure

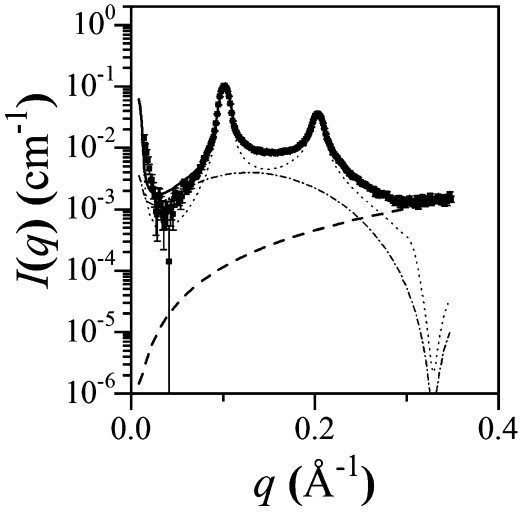

Figure 7. Experimental SAXS data for 2 wt % pure DMPC solution given as squares. Solid line is the fit by model 4 (multilayer + bilayer), dotted line is the contribution from multilayers, dashed dotted line is the contribution from bilayers, and dashed line is the background contribution.

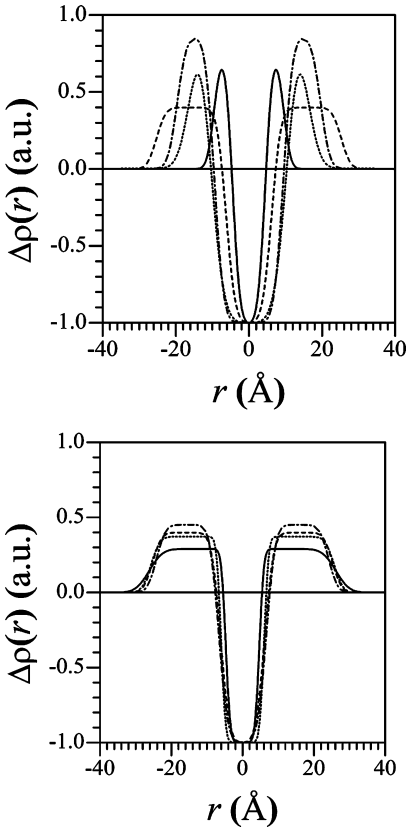

Figure 8. Contrast, $\Delta\rho$, of structures under the condition where the contrast in the core is set to −1. Top: DHPC (solid line), Q = 0.5 (dotted line), Q = 3.2 (dashed line), and DMPC (dashed dotted line). Bottom: Q = 1 (solid line), Q = 2 (dotted line), Q = 3.2 (dashed line), and Q = 4 (dashed dotted line).

displays a longer-range order, which results from the ability of DMPC bilayers to stack into multilayers.[46] The data are fitted by model 4, consisting of a multilayered structure together with free bilayers. The model does not attempt to describe the overall structure of the multilayers, for example, vesicles, as the overall size extends beyond the largest size that can be resolved from the SAXS experiment. Therefore, there is some discrepancy between model and data at low q (Figure 7). The model fit results give an average number of layers in the multilayer structure, N = 10.7 ± 0.2, a half-width of the bilayer core, W_c, of 9.1 ± 0.4 Å, a shell thickness of D_W = 12.3 ± 0.6 Å, and a distance between the bilayers in the multilayer of d = 61.7 ± 0.1 Å. The smearing widths of the core−shell and shell−solvent interfaces were both fixed at 2.0 Å. These results and the contrast profile (Figure 8, top) are in good agreement with results from Kučerka et al.,[47] considering that the resolution of the data in the present work is considerably lower. All model parameters and errors are given in Table 1.

Bilayer Cross Section Profiles. The resulting profiles are shown in Figure 8. The central core is narrowest for the pure DHPC sample as expected, and it is largest for Q = 0.5 and pure DMPC (Figure 8 top). The headgroup shell thickness is smallest for pure DHPC and Q = 0.5, slightly larger for pure DMPC, and significantly larger for the mixture with values of Q from 1 to 4 (Figure 8 bottom). The thick shells occur for the samples with significant amounts of DMPC. The thickness is larger than what can be expected for a lipid headgroup, where only the phosphatidyl part contributes, which suggests, as mentioned previously, some degree of mixing of DHPC and DMPC in these areas, which leads to disorder and staggering of the molecules. The staggering is further supported by the fact that the core is smaller for the mixed samples as compared to pure DMPC.

Distribution of DHPC and DMPC in Structures. Modeling of SAXS data gives a number of results on the structure and aggregation numbers, N_{agg}, of the aggregates. The area per headgroup, A_{head}, can be estimated from these results by calculating the surface area of the core of the models and dividing it by the aggregation number. Because of the similar chemical structure of the DHPC and the DHPC molecules, it is a reasonable assumption that the headgroup area is the same for the two types of molecules. The number of molecules used for covering the rim can be calculated as the area of the rim divided by A_{head}. According to the classical bicelle models, these lipids are DHPC, which has a larger preferred curvature compared to DMPC. This results in a derived number of DHPC molecules in the rim, $N_{DHPC,rim}$. The rest of the DHPC molecules, $N_{DHPC,flat}$, and the total number of DMPC molecules, N_{DMPC}, then cover the flat parts of the structure. From the definition of Q, the number of DHPC molecules per aggregate is $N_{DHPC} = N_{agg}/(1 + Q)$, so that $N_{DHPC,flat} = N_{DHPC} - N_{DHPC,rim}$. The number of DMPC molecules per aggregate is $N_{DMPC} = N_{agg}Q/(1 + Q)$. Note that the relative distribution of the molecules is independent of the value used for the area per

DOI: 10.1021/acs.langmuir.8b02704
Langmuir 2018, 34, 14597−14607

headgroup and that only the specific numbers per micelle are dependent on the used value.

The results for the derived parameters are given in Table 3 together with the fraction of DHPC molecules in the flat part

Table 3. Headgroup Area and Molecular Distributions Derived from the Modeling Results

Q	0	0.5	1.0	2.0	3.2	4.0
A_{head} (Å^2)	104	68	97	70	64	92
$N_{DHPC,rim}$		33	33	98	170	129
$N_{DHPC,flat}$		11	46	64	78	102
N_{DMPC}		22	79	325	793	921
f		0.33	0.37	0.16	0.09	0.10

of the bilayer, $f = N_{DHPC,flat}/(N_{DHPC,flat} + N_{DMPC})$. Uncertainties are not given as they would likely be dominated by systematic errors, like uncertainty on the absolute scale of the SAXS intensities (5−10%), on the contrast (of similar magnitude) and errors originating from the idealized models with sharp edges and corners. The uncertainty on the headgroup area is therefore about 15−20% and for the fraction f for DHPC molecules in the flat areas, it is about 30%.

The headgroup area is in the range 64−104 Å^2, so the headgroup areas are in general similar or larger than the value of 60 Å^2 determined for pure DMPC bilayers.[47,48]

The fraction of DHPC molecules in the flat area for low Q is quite large (about 35%). It was not expected for Q = 0.5, where the shell is quite narrow and well defined, which suggests that the molecules mix but not cause significant disorder at this composition. The fraction decreases for increasing values of Q and reaches about 10% for Q = 3.2 and 4.0. These relatively large fractions are in agreement by coarse-grained molecular dynamics (MD) simulations,[48] which show a large degree of mixing in bicelles with Q = 0.5 and a lower degree of mixing at Q = 3.2 with f = 12% in excellent agreement with the present results. However, there are also discrepancies between the present results and the MD simulations. For Q = 0.5, the MD simulations show large variations in shape, size, and composition, which is not supported by the SAXS results. In general, the structures obtained by MD are larger than those found in the present work. However, part of this deviation might be explained by the lower concentration of lipids in the experimental system as compared to the MD simulations, as higher concentration in general induced growth in the size of self-assembled structures.[49]

CONCLUSIONS

SAXS data were collected for dilute solutions of DHPC and DMPC as well as a range of mixtures with different mixing ratios, Q. In order to avoid changes in the value of Q in the bicelles due to draining of the soluble DHPC from the bicelles upon dilution, they were diluted with solutions containing a certain concentration of DHPC. This concentration was determined for each mixing ratio Q as the concentration for which dilution would not alter the minimum of the scattering form factor and thereby the bicelle structure and composition. This DHPC concentration is 9, 5, 5, 4.5, and 4.5 mM for Q = 0.5, 1, 2, 3.2, and 4, respectively.

The scattering data for dilute samples of lipid concentration 2 wt % were modeled on absolute scale (except pure DMPC data, which were modeled on arbitrary scale) to obtain the shape and size of the lipid aggregates. For pure DHPC aggregates, the data could be modeled as small core−shell ellipsoids with an aggregation number of 16 and a thin headgroup shell. At Q = 0.5, the lipids form core−shell aggregates with the shape of disks (modeled as short, tablet-shaped cylinders) with an aggregation number of 66 and also with a narrow headgroup shell. For Q = 1, 2, 3.2, and 4, the data could be modeled using a shape of rectangular cuboids, which increase in size (particularly in the long direction) with increasing mixing ratio Q. These structures had a significantly larger thickness of headgroup layer on the flat parts compared to the pure systems of DHPC and DMPC. Pure DMPC in aqueous solution forms multilamellar structures of around 11 bilayers together with free bilayers, where the headgroup thickness is lower than that of the mixtures. An overview of the formed aggregates can be seen in Figure 9.

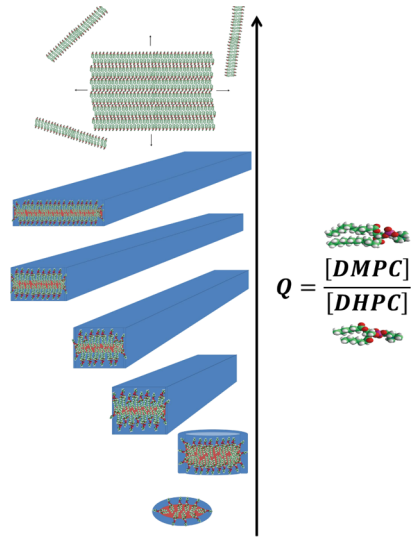

Figure 9. Overview of bicelle morphologies as a function of Q. The drawing is not to scale.

The structural determinations in the present work at 37 °C in pure water show that the morphology as a function of Q does not follow the ideal bicelle model as proposed by Prosser and Vold.[2] The structure of the ideal model is a round disk, where pure DMPC forms the flat areas and DHPC is entirely located at the rim. For all DMPC/DHPC mixing ratios, the lipids were shown to form flat aggregates with bilayers that grow in size in one or two of the lateral directions as a function of Q. The larger thickness of the headgroup shell of the structures with Q in the range from 1 to 4 suggests that there is some degree of mixing of DHPC into the flat areas of the structures, which causes disorder and staggering of the molecules. Despite the hydrophobic−hydrophilic mismatch caused between the DHPC and DMPC molecules, there might also be gain in the electrostatic energy as staggering brings the positively charged choline group of DHPC closer to the negatively charged phosphatidyl group of the DMPC. The intermixing is further supported by the estimation of the distribution of molecules from the areas of the flat parts and of the rim with about one-third DHPC for Q = 0.5 and 1, decreasing to ca. 10% for Q = 3.2 and 4. Such intermixing of DHPC into the flat areas is favored by the mixing entropy but limited because of the curvature that the short DHPC induces when inserted into the flat regions and the elastic bending energy associated with this.[50] It is also limited because of the

DOI: 10.1021/acs.langmuir.8b02704
Langmuir 2018, 34, 14597−14607

lower number of bicelles that results from having fewer DHPC for covering the rim, as the lower number of bicelles reduces the contribution to the entropy of mixing of the bicelles with the solvent.

The change in shape and growth in the various directions can be explained by the theory of Bergström,[51] which analyses the bending energetics of the aggregates. The theory involves three bending elasticity constants: the spontaneous curvature, the bending rigidity, and the saddle-splay constant. Globular micelles or cylinders are formed for larger bending rigidities, whereas various bilayer structures like tablet-shaped or ribbon-like micelles are present for lower bending rigidities. The width or the radius of these is mainly decided by the spontaneous curvature and the saddle-splay constant primarily determines the overall size but does not influence the shape of the aggregates. As the Q value is changed for the bicelles and intermixing of short-chain DHPC into the flat areas occurs, it is plausible that there is a gradual change of the elastic constants, so that the structures change gradually from globular micelles, over cuboidal structure, to more extended bilayers, as observed experimentally.

The contrast conditions in SAXS with positive and negative contrast of core and shell of the bicelles, respectively, make it particularly challenging to model the SAXS data compared to the SANS data, where the contrast without specific deuteration of part of the molecules has the same sign for core and shell. This is probably the reason that despite several publications in the literature in which SAXS is applied to bicellar systems,[52−54] there is to our knowledge only one previous publication, where modeling was done[53] for bicelles of 1,2-dipalmitoyl-*sn*-glycero-3-phosphocholine and 1,2-diheptanoyl-*sn*-glycero-3-phosphocholine at a composition of $Q = 3$. However, when SAXS data are modeled on absolute scale using molecular, composition, and concentration constraints as done in the present work, it provides quite detailed information on the structure and organization of the constituting molecules. Such detailed information can only be obtained by SANS when the lipid molecules are selectively deuterated.

■ ASSOCIATED CONTENT

Supporting Information

The Supporting Information is available free of charge on the ACS Publications website at DOI: 10.1021/acs.langmuir.8b02704.

Models and an overview of all scattering data (PDF)

■ AUTHOR INFORMATION

Corresponding Author

*E-mail: jsp@chem.au.dk.

ORCID

Thomas Vosegaard: 0000-0001-5414-4550

Jan Skov Pedersen: 0000-0002-7768-0206

Present Address

†NIST, Center for Neutron Research, Gaithersburg, MD 20899 USA.

Notes

The authors declare no competing financial interest.

■ ACKNOWLEDGMENTS

This work was supported by grants from the Lundbeck Foundation and the Danish Council for Independent Research Natural Sciences (4002-00479B—FNU).

■ ABBREVIATIONS

cmc, critical micelle concentration; DHPC, dihexanoyl phosphatidyl choline; DMPC, dimyristoyl phosphatidyl choline; IFT, indirect Fourier transformation; MD, molecular dynamics; NMR, nuclear magnetic resonance; SAXS, small-angle X-ray scattering; SLDD, scattering length density difference

■ REFERENCES

(1) Sanders, C. R.; Landis, G. C. Reconstitution of Membrane Proteins into Lipid-Rich Bilayered Mixed Micelles for NMR Studies. *Biochemistry* **1995**, *34*, 4030−4040.

(2) Vold, R. R.; Prosser, R. S. Magnetically oriented phospholipid bilayered micelles for structural studies of polypeptides. Does the ideal bicelle exist? *J. Magn. Reson., Ser. B* **1996**, *113*, 267−271.

(3) van Dam, L.; Karlsson, G.; Edwards, K. Direct observation and characterization of DMPC/DHPC aggregates under conditions relevant for biological solution NMR. *Biochim. Biophys. Acta, Biomembr.* **2004**, *1664*, 241−256.

(4) Israelachvili, J. N.; Mitchell, D. J.; Ninham, B. W. Theory of Self-Assembly of Hydrocarbon Amphiphiles into Micelles and Bilayers. *J. Chem. Soc., Faraday Trans. 2* **1976**, 1525−1568.

(5) Prosser, R. S.; Evanics, F.; Kitevski, J. L.; Al-Abdul-Wahid, M. S. Current Applications of Bicelles in NMR Studies of Membrane-Associated Amphiphiles and Proteins. *Biochemistry* **2006**, *45*, 8453−8465.

(6) Harroun, T. A.; Koslowsky, M.; Nieh, M.-P.; de Lannoy, C.-F.; Raghunathan, V. A.; Katsaras, J. Comprehensive examination of mesophases formed by DMPC and DHPC mixtures. *Langmuir* **2005**, *21*, 5356−5361.

(7) Bolze, J.; Fujisawa, T.; Nagao, T.; Norisada, K.; Saitô, H.; Naito, A. Small angle X-ray scattering and 31P NMR studies on the phase behavior of phospholipid bilayered mixed micelles. *Chem. Phys. Lett.* **2000**, *329*, 215−220.

(8) van Dam, L.; Karlsson, G.; Edwards, K. Morphology of Magnetically Aligning DMPC/DHPC Aggregates Perforated Sheets, Not Disks. *Langmuir* **2006**, *22*, 3280−3285.

(9) Pedersen, J. S. A flux- and background-optimized version of the NanoSTAR small-angle X-ray scattering camera for solution scattering. *J. Appl. Crystallogr.* **2004**, *37*, 369−380.

(10) Li, Y.; Beck, R.; Huang, T.; Choi, M. C.; Divinagracia, M. Scatterless hybrid metal-single-crystal slit for small-angle X-ray scattering and high-resolution X-ray diffraction. *J. Appl. Crystallogr.* **2008**, *41*, 1134−1139.

(11) Orthaber, D.; Bergmann, A.; Glatter, O. SAXS experiments on absolute scale with Kratky systems using water as a secondary standard. *J. Appl. Crystallogr.* **2000**, *33*, 218−225.

(12) Glatter, O. A new method for the evaluation of small-angle scattering data. *J. Appl. Crystallogr.* **1977**, *10*, 415−421.

(13) Pedersen, J. S.; Hansen, S.; Bauer, R. The aggregation behavior of zinc-free insulin studied by small-angle neutron scattering. *Eur. Biophys. J. Biophys. Lett.* **1994**, *23*, 227−229.

(14) Nieh, M.-P.; Glinka, C. J.; Krueger, S.; Prosser, R. S.; Katsaras, J. SANS study on the effect of lanthanide ions and charged lipids on the morphology of phospholipid mixtures. *Biophys. J.* **2002**, *82*, 2487−2498.

(15) Nieh, M.-P.; Raghunathan, V. A.; Glinka, C. J.; Harroun, T. A.; Pabst, G.; Katsaras, J. Magnetically Alignable Phase of Phospholipid "Bicelle" Mixtures Is a Chiral Nematic Made Up of Wormlike Micelles. *Langmuir* **2004**, *20*, 7893−7897.

(16) Guinier, A. La diffraction des rayons X aux très petits angles : application à l'étude de phénomènes ultramicroscopiques. *Ann. Phys.* **1939**, *11*, 161−237.
(17) Mittelbach, P.; Porod, G. Röntgenkleinwinkelstreuung verdünnter kolloider Systeme VI. *Acta Phys. Austriaca* **1961**, *14*, 405−439.
(18) Mittelbach, P.; Porod, G. Zur Röntgenkleinwinkelstreuung verdünner kolloider Systeme. Die Berechnung der Streukurven von parallelepipeden. *Acta Phys. Austriaca* **1961**, *14*, 185−211.
(19) Cates, M. E.; Candau, S. J. Statics and Dynamics of Worm-Like Surfactant Micelles. *J. Phys.: Condens. Matter* **1990**, *2*, 6869−6892.
(20) Pabst, G.; Rappolt, M.; Amenitsch, H.; Laggner, P. Structural information from multilamellar liposomes at full hydration: Full q-range fitting with high quality x-ray data. *Phys. Rev. E: Stat. Phys., Plasmas, Fluids, Relat. Interdiscip. Top.* **2000**, *62*, 4000−4009.
(21) Kratky, O. G.; Glatter, O. *Small Angle X-ray Scattering*; Academic Press: London, 1982.
(22) Opella, S. J.; Marassi, F. M. Structure determination of membrane proteins by NMR spectroscopy. *Chem. Rev.* **2004**, *104*, 3587−3606.
(23) Triba, M. N.; Warschawski, D. E.; Devaux, P. F. Reinvestigation by phosphorus NMR of lipid distribution in bicelles. *Biophys. J.* **2005**, *88*, 1887−1901.
(24) Bertelsen, K.; Dorosz, J.; Hansen, S. K.; Nielsen, N. C.; Vosegaard, T. Mechanisms of Peptide-Induced Pore Formation in Lipid Bilayers Investigated by Oriented P-31 Solid-State NMR Spectroscopy. *PLoS One* **2012**, *7*, No. e47745.
(25) Hansen, S. K.; Vestergaard, M.; Thøgersen, L.; Schiøtt, B.; Nielsen, N. C.; Vosegaard, T. Lipid Dynamics Studied by Calculation of 31P Solid-State NMR Spectra Using Ensembles from Molecular Dynamics Simulations. *J. Phys. Chem. B* **2014**, *118*, 5119−5129.
(26) Hansen, S. K.; Bertelsen, K.; Paaske, B.; Nielsen, N. C.; Vosegaard, T. Solid-state NMR methods for oriented membrane proteins. *Prog. Nucl. Magn. Reson. Spectrosc.* **2015**, *88*−*89*, 48−85.
(27) Sanders, C. R.; Prosser, R. S. Bicelles: a model membrane system for all seasons? *Structure* **1998**, *6*, 1227−1234.
(28) Lindblom, G.; Rilfors, L. Cubic phases and isotropic structures formed by membrane lipids - possible biological relevance. *Biochim. Biophys. Acta* **1989**, *988*, 221−256.
(29) Park, S. H.; De Angelis, A. A.; Nevzorov, A. A.; Wu, C. H.; Opella, S. J. Three-dimensional structure of the transmembrane domain of Vpu from HIV-1 in aligned phospholipid bicelles. *Biophys. J.* **2006**, *91*, 3032−3042.
(30) Bain, A. D. Chemical exchange in NMR. *Prog. Nucl. Magn. Reson. Spectrosc.* **2003**, *43*, 63−103.
(31) Tausk, R. J. M.; Oudshoorn, C.; Overbeek, J. T. G. Physical chemical studies of short-chain lecithin homologues. *Biophys. Chem.* **1974**, *2*, 53−63.
(32) Burns, R. A.; Roberts, M. F.; Dluhy, R.; Mendelsohn, R. Monomer-to-micelle transition of dihexanoylphosphatidylcholine: carbon-13 NMR and Raman studies. *J. Am. Chem. Soc.* **1982**, *104*, 430−438.
(33) Ottiger, M.; Bax, A. Characterization of magnetically oriented phospholipid micelles for measurement of dipolar couplings in macromolecules. *J. Biomol. NMR* **1998**, *12*, 361−372.
(34) Chou, J. J.; Baber, J. L.; Bax, A. Characterization of phospholipid mixed micelles by translational diffusion. *J. Biomol. NMR* **2004**, *29*, 299−308.
(35) Glover, K. J.; Whiles, J. A.; Wu, G.; Yu, N.-j.; Deems, R.; Struppe, J. O.; Stark, R. E.; Komives, E. A.; Vold, R. R. Structural evaluation of phospholipid bicelles for solution-state studies of membrane-associated biomolecules. *Biophys. J.* **2001**, *81*, 2163−2171.
(36) Lipfert, J.; Columbus, L.; Chu, V. B.; Lesley, S. A.; Doniach, S. Size and shape of detergent micelles determined by small-angle x-ray scattering. *J. Phys. Chem. B* **2007**, *111*, 12427−12438.
(37) Lin, T. L.; Chen, S. H.; Gabriel, N. E.; Roberts, M. F. The use of small-angle neutron scattering to determine the structure and interaction of dihexanoylphosphatidylcholine micelles. *J. Am. Chem. Soc.* **1986**, *108*, 3499−3507.
(38) Vass, S.; Pedersen, J. S.; Pleštil, J.; Laggner, P.; Rétfalvi, E.; Varga, I.; Gilányi, T. Ambiguity in determining the shape of alkali alkyl sulfate micelles from small-angle scattering data. *Langmuir* **2008**, *24*, 408−417.
(39) Ye, W.; Lind, J.; Eriksson, J.; Mäler, L. Characterization of the Morphology of Fast-Tumbling Bicelles with Varying Composition. *Langmuir* **2014**, *30*, 5488−5496.
(40) Sanders, C. R.; Schwonek, J. P. Characterization of Magnetically Orientable Bilayers in Mixtures of Dihexanoylphosphatidylcholine and Dimyristoylphosphatidylcholine by Solid-State Nmr. *Biochemistry* **1992**, *31*, 8898−8905.
(41) De Angelis, A. A.; Opella, S. J. Bicelle samples for solid-state NMR of membrane proteins. *Nat. Protoc.* **2007**, *2*, 2332−2338.
(42) Sternin, E.; Nizza, D.; Gawrisch, K. Temperature dependence of DMPC/DHPC mixing in a bicellar solution and its structural implications. *Langmuir* **2001**, *17*, 2610−2616.
(43) Wu, H.; Su, K.; Guan, X.; Sublette, M. E.; Stark, R. E. Assessing the size, stability, and utility of isotropically tumbling bicelle systems for structural biology. *Biochim. Biophys. Acta, Biomembr.* **2010**, *1798*, 482−488.
(44) Sanders, C. R.; Hare, B. J.; Howard, K. P.; Prestegard, J. H. Magnetically-Oriented Phospholipid Micelles as a Tool for the Study of Membrane-Associated Molecules. *Prog. Nucl. Magn. Reson. Spectrosc.* **1994**, *26*, 421−444.
(45) Uddin, M. N.; Morrow, M. R. Bicellar Mixture Phase Behavior Examined by Variable-Pressure Deuterium NMR and Ambient Pressure DSC. *Langmuir* **2010**, *26*, 12104−12111.
(46) Somerharju, P.; Virtanen, J. A.; Cheng, K. H. Lateral organisation of membrane lipids. *Biochim. Biophys. Acta, Mol. Cell Biol. Lipids* **1999**, *1440*, 32−48.
(47) Kučerka, N.; Liu, Y.; Chu, N. J.; Petrache, H. I.; Tristram-Nagle, S. T.; Nagle, J. F. Structure of fully hydrated fluid phase DMPC and DLPC lipid bilayers using X-ray scattering from oriented multilamellar arrays and from unilamellar vesicles. *Biophys. J.* **2005**, *88* (4), 2626−2637.
(48) Vestergaard, M.; Kraft, J. F.; Vosegaard, T.; Thøgersen, L.; Schiøtt, B. Bicelles and Other Membrane Mimics: Comparison of Structure, Properties, and Dynamics from MD Simulations. *J. Phys. Chem. B* **2015**, *119*, 15831−15843.
(49) Jones, R. A. L. *Soft Condensed Matter*; Oxford University Press: Oxford, New York, 2002; p 195.
(50) Israelachvili, J. N.; Mitchell, D. J.; Ninham, B. W. Theory of Self-Assembly of Lipid Bilayers and Vesicles. *Biochim. Biophys. Acta* **1977**, *470*, 185−201.
(51) Bergström, L. M. Bending energetics of tablet-shaped micelles: A novel approach to rationalize micellar systems. *ChemPhysChem* **2007**, *8*, 462−472.
(52) Kozak, M.; Domka, L.; Jurga, S. The effect of selected surfactants on the structure of a bicellar system (DMPC/DHPC) studied by SAXS. *J. Mol. Struct.* **2007**, *846*, 108−111.
(53) Yang, P. W.; Lin, T. L.; Hu, Y.; Jeng, U. S. Small-Angle X-ray Scattering Studies on the Structure of Mixed DPPC/diC(7)PC Micelles in Aqueous Solutions. *Chin. J. Phys.* **2012**, *50*, 349−356.
(54) Jeworrek, C.; Uelner, S.; Winter, R. Phase behavior and kinetics of pressure-jump induced phase transitions of bicellar lipid mixtures. *Soft Matter* **2011**, *7*, 2709−2719.

DOI: 10.1021/acs.langmuir.8b02704
Langmuir 2018, 34, 14597−14607